Radially biased diffusion-limited aggregation

Paul Meakin
Central Research and Development Department, E. I. du Pont de Nemours and Company, Wilmington, Delaware 19880-0356 and Department of Physics, University of Oslo, Box 1048, Blindern, 0316 Oslo 3, Norway

Jens Feder and Torstein Jøssang
Department of Physics, University of Oslo, Box 1048, Blindern, 0316 Oslo 3, Norway
(Received 26 July 1990)

A series of random growth models has been studied in which the growth probability at position $\mathbf{r}$ on the surface of the growing cluster is given by $P(\mathbf{r})\simeq\mu(\mathbf{r})l^{\phi}$, where $\mu(\mathbf{r})$ is the harmonic measure at $\mathbf{r}$ and l is the distance from the seed or origin. The distance l can be either the Pythagorean distance or the minimum path distance measured on the growing cluster. The introduction of this scale-invariant perturbation of the usual diffusion-limited-aggregation (DLA) model ($\phi=0$) introduces a distance-dependent correlation length, $\xi=l/|\phi|$, that characterizes a geometrical crossover in the cluster structure. Although the structures generated by these models have an appearance that is quite different from that of DLA clusters (for $|\phi|\gg 0$), the growth of their radii of gyration and the internal density profile $\rho(r)$ have simple power-law forms with the same exponents as those associated with DLA. The difference in scaling is manifest in the amplitudes of the power-law forms. These amplitudes exhibit a power-law dependence on the radial bias exponent ϕ. For $\phi\gg 1$ the clusters become self-affine structures with the same exponents as those associated with DLA on length scales $r\ll\xi$. These clusters exhibit a crossover to self-affine wedgelike linearly growing structures at $r\simeq\mathcal{R}_x\simeq\phi$. For $\phi\ll -1$ the growth probability is enhanced in the core of the clusters. These clusters exhibit a dense core having radius $\mathcal{R}_x\sim|\phi|$. For $r\simeq\mathcal{R}_x$, the structure crosses over to a structure having the same scaling behavior as DLA. For growth from a line in a strip of width L, the density-density correlation function in the lateral direction can be represented by the scaling form $C_h(x)\sim\xi^{-\alpha}g(x/\xi^{\alpha/\nu})$, where h is the distance from the line substrate (height) and exponents α and ν have values of about $\frac{1}{3}$ and $\frac{1}{2}$, respectively. The scaling function $g(x)$ has the form $g(x)\simeq x^{-\nu}$ for $x\ll 1$ and $g(x)\sim$ const for $x\gg 1$.

I. INTRODUCTION

Even though the diffusion-limited-aggregation (DLA) model of Witten and Sander[1] is still not well understood from a fundamental point of view, it has been used successfully to describe a wide range of nonequilibrium growth processes including electrodeposition, dielectric breakdown, fluid-fluid displacement processes, the dissolution of porous materials, random dendritic growth, and a variety of biological growth processes. A description of these applications can be found in Refs. 2–10 and in the original literature cited in these references. In all these cases highly ramified fractal[11] patterns are formed that closely resemble those generated by the DLA model. The striking similarity between the patterns generated by these apparently diverse growth processes is a consequence of a common underlying growth mechanism controlled by growth probabilities that are determined by a scalar field obeying the Laplace equation, $\nabla^2\mu=0$, with absorbing boundary conditions at the growing interface and a fixed value for μ at "infinity." The growth probability $\mu(\mathbf{r})$ is also the *harmonic measure* of the growing structure.

In many systems a relatively small change in the growth conditions[12–22] leads to patterns that are quite different from DLA and the origins of these patterns are poorly understood. Since these diverse growth processes appear to be quite closely related to DLA, they have stimulated further investigations[23–33] of a variety of growth models closely related to DLA. In the original DLA model[1] the growth probability at position $\mathbf{r}$ on the surface of the growing structure is proportional to the harmonic measure $\mu(\mathbf{r})$ (or its gradient normal to the surface). In most DLA models the Laplacian field is simulated using random walks. Here we explore the patterns generated by a simple modification of the DLA model in which the growth probability $P(\mathbf{r})$ at position $\mathbf{r}$ is given by the product of the harmonic measure $\mu(\mathbf{r})$ at the growth site and a statistically independent power-law radial bias acceptance probability l^{ϕ}:

$$P(\mathbf{r})\simeq\mu(\mathbf{r})l^{\phi}\text{ with }\begin{cases} l=|\mathbf{r}-\mathbf{r}_0|, & \text{model I}\\ l=d(\mathbf{r}), & \text{model II}\end{cases}. \tag{1}$$

In Eq. (1) $l=l(\mathbf{r})$ is the distance from the position $\mathbf{r}$ to the position $\mathbf{r}_0$ of the "seed" or origin. This distance is either simply the Pythagorean distance (model I) or the minimum path distance $d(\mathbf{r})$ from the position $\mathbf{r}$ on the growing surface to the origin measured *on* the growing cluster (model II). Note that the DLA model is

recovered in model I, as the radial bias exponent vanishes, i.e., $\phi=0$.

These models were motivated by the idea that for some (particularly biological) systems[34] the growth probability might depend on the distance from the growth sites to the origin as well as on the magnitude of the Laplacian field (concentration of nutrient or toxic waste products, for example). It also seemed probable that this simple model might provide insight into other growth processes, particularly those leading to the formation of "dense radial" patterns ($\phi<0$) and patterns more tenuous than DLA ($\phi>0$).

This work was also motivated by the results of simulations[4] in which DLA clusters were probed using particles that followed random walk trajectories that were terminated on contact with the cluster. Such simulations provide an estimate of the harmonic measure $\mu(\mathbf{r})$ or growth probability measure on the surface of the cluster.

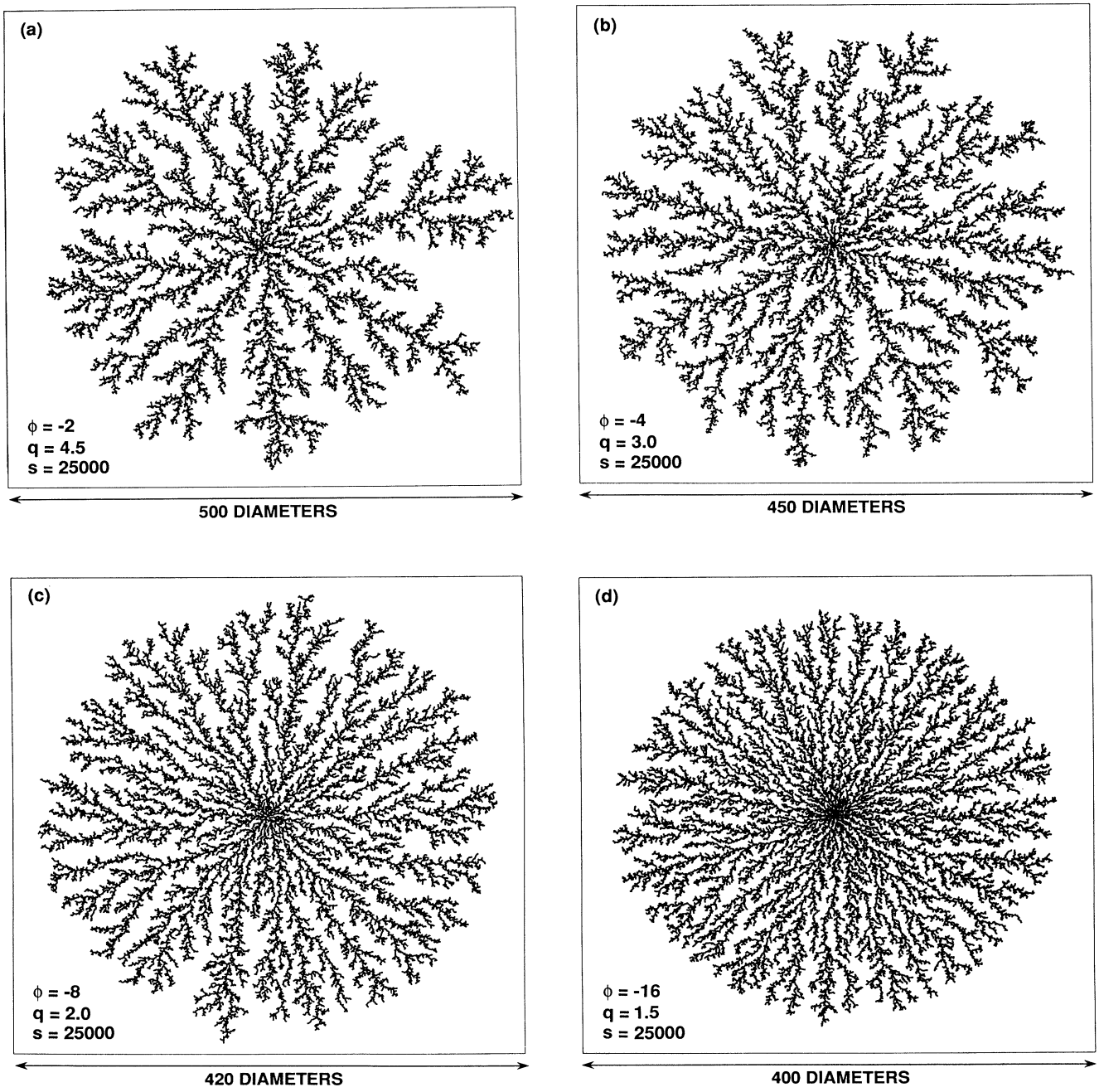

FIG. 1. Clusters of 25 000 particles generated using an off-lattice version of model I ($l=|\mathbf{r}-\mathbf{r}_0|$) with negative values of the exponent ϕ. (a), (b), (c), and (d) show clusters generated with $\phi=-2$, -4, -8, and -16, respectively.

The number of contacts at a distance $|\mathbf{r}-\mathbf{r}_0|$ in the range $[R, R+\delta R]$ was found to be given by $N(R)\delta R$ where $N(R)\sim R^{\delta}$ and the exponent δ had a value of about 8.1 for interior regions of the cluster. It appears reasonable to suppose that this exponent is characteristic of the growth process and that the models explored here might change this exponent and the fractal scaling properties of the clusters.

II. COMPUTER MODELS

The models used in this work were based on efficient two-dimensional off-lattice and square-lattice DLA models.[35,36] In the simplest version of these models random walkers are launched, one at a time, from outside of the region occupied by the cluster. When a particle contacts the cluster the distance l [i.e. $|\mathbf{r}-\mathbf{r}_0|$ or $d(\mathbf{r})$] from the

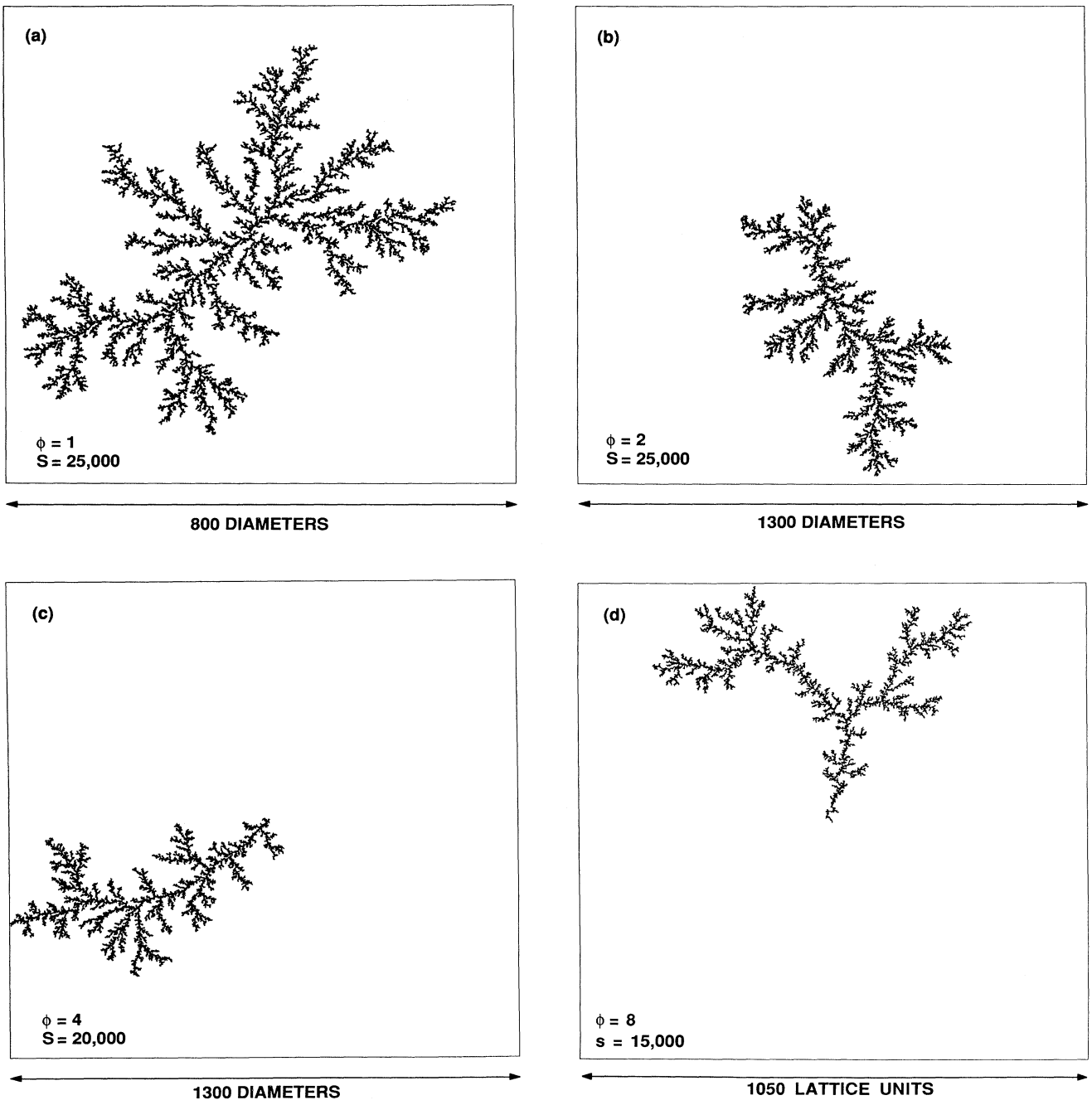

FIG. 2. Off-lattice clusters grown using model II [$l=d(\mathbf{r})$] with positive values of the exponent ϕ in Eq. (1). (a), (b), (c), and (d) show clusters generated with $\phi=1$, 2, 4, and 8, respectively. Each cluster started growing at the center of the square box that surrounds it.

center of the contacting particle to the origin is calculated. If the radial bias exponent ϕ is positive then the particle is incorporated into the cluster at its position of contact if a random number x uniformly distributed over the range $0<x<1$ is smaller than $(l/l_m)^{\phi}$. Here l_m is the largest possible value for l. If the particle is not incorporate into the cluster, the random walk trajectory is terminated and a new random walk is launched from a random position of the launching circle that just encloses the cluster. The process described above is repeated many times until a sufficiently large cluster has been generated.

If the radial bias exponent $\phi<0$ in Eq. (1), the contacting particle can be incorporated into the cluster if $x<(ql/l_m)^{\phi}$ where the parameter q is selected to be sufficiently large so that $(ql/l_m)^{\phi}$ is (almost) always smaller than 1. Correct results are obtained by choosing q sufficiently large. However, in practice care must be exercised in selecting the appropriate value of q since a value that is too large will lead to very inefficient simulations and a value that is too small will lead to systematic errors. For $\phi>0$ we may set $q=1$ since $(l/l_m)^{\phi}$ is always smaller than 1.

For the off-lattice DLA clusters there are no loops and the distance d is the length of the nonreentrant path from the center of the contacting particle to the origin consisting of vectors between the centers of contacting particles in the cluster. For the square-lattice model small loops do occur and the distance d is the minimum path consisting of vectors contacting the centers of nearest-neighbor lattice sites.

III. RESULTS

Most of the simulations were carried out using the off-lattice models. Figure 1 shows four clusters generated using the off-lattice version of model I [Eq. (1), $l=|\mathbf{r}-\mathbf{r}_0|$]. Values of -2, -4, -8, and -16 were used for the exponent ϕ and the corresponding values for the parameter q were 4.5, 3.0, 2.0, and 1.5, respectively. Very similar patterns were obtained using model II. Similarly, Fig. 2 shows clusters generated using model II with four different positive values of the exponent ϕ in Eq. (1) ($\phi=1$, 2, 4, and 8). The clusters shown in Figs. 1 and 2 (particularly for large positive and negative values of ϕ) have a quite different appearance than ordinary DLA clusters. Figure 3 shows quite extreme examples (a cluster of 10^5 particles grown using an off-lattice version of model I with $\phi=-32$ and $q=1.2$ and a cluster grown using the same model with $\phi=16$). In qualitative terms the cluster in Fig. 3(a) looks more like a dense radial pattern than a DLA pattern.

A. Scaling of the radius of gyration

To obtain a more quantitative description of the cluster geometry the dependence of radius of gyration R_g on the cluster size or number of particles s was measured. Figure 4 shows the dependence of $\ln(R_g/s^{(1/1.7)})$ on $\ln(s)$ obtained from clusters generated using model I with $\phi=-8$ and three different values for the parameter q. At least 20 clusters were used for each value of q. It is apparent from Fig. 4 that as the value of the parameter q is increased the systematic uncertainties due to the use of a finite value for q decrease; the dependence of R_g on s converges and the asymptotic dependence of R_g on s can be written in the form

$$R_g=R_0(\phi)s^{\beta}, \tag{2}$$

where $\beta=1/D_{\beta}$ and D_{β} has a value close to 1.70. Similarly, results were obtained for model II with $\phi=-8$ and

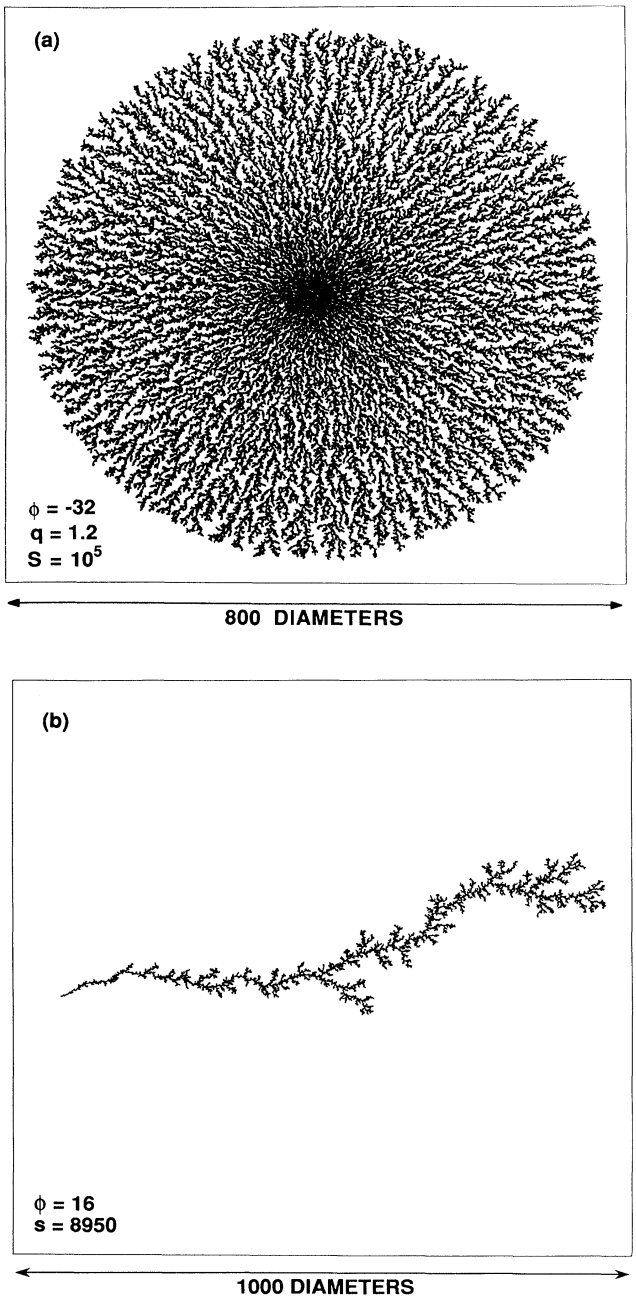

FIG. 3. (a) shows a 100 000 particle cluster grown using an off-lattice version of model I with $\phi=-32$ and $q=1.2$. 3(b) shows a cluster of particles using the same model with $\phi=16$.

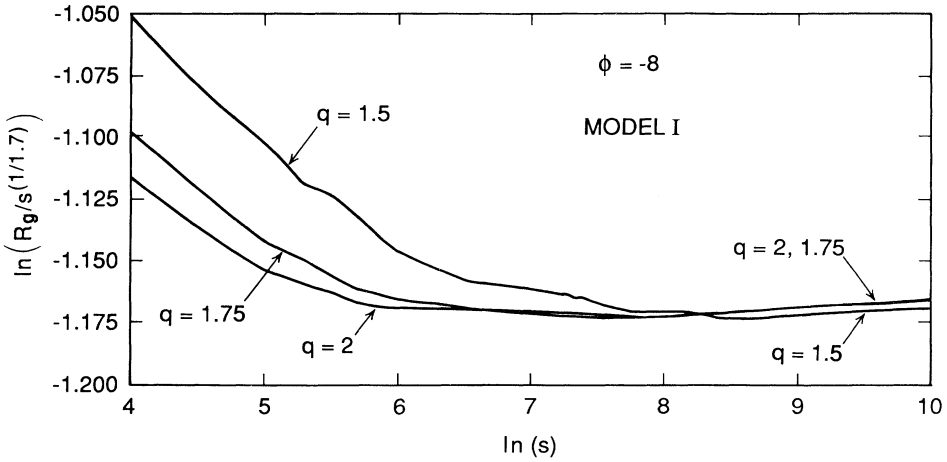

FIG. 4. Dependence of $\ln(R_g/s^{(1/1.7)})$ on $\ln(s)$ obtained from model I simulations with a radial bias exponent $\phi=-8$. Results are given for three different values of q to illustrate the rapid convergence with increasing q.

for both models I and II with $\phi=-16$. For $\phi=-2$ and -4, it is possible to use sufficiently large values for q that uncertainties due to finite q can be reduced to negligible proportions without seriously compromising the efficiency of the simulations.

Figure 5 shows the dependence of $\ln(R_g/s^{(1/1.7)})$ on $\ln(s)$ obtained from simulations carried out with eight different values for the exponent ϕ using model II. It is apparent from this figure that the dependence of the cluster radii of gyration on cluster size can be described quite well by Eq. (2) with a value of about $\frac{1}{1.70}$ for the exponent β. In this case the clusters generated using all the values of ϕ have a fractal dimensionality D_β of 1.70±0.03. This value is the same (within statistical and systematic uncertainties) as that of ordinary off-lattice DLA (Ref. 35) ($D_\beta=1.715\pm0.004$).

B. Scaling of the cluster mass $N(r)$

A method that is frequently used to estimate the fractal dimensionality of clusters grown from a seed is to measure the number of particles $N(r)$ within a distance r from the seed or origin.

For a fractal structure we expect to find that

$$N(r)=N_0(\phi)r^{D_\gamma}, \tag{3}$$

for distances $r\gg1$ (i.e., the particle diameter) and $r\ll R_g$. Figure 6(a) shows the dependence of $\ln[N(r)/r^{1.70}]$ on $\ln(r)$ obtained from model II off-lattice simulations with five negative values for the radial bias exponent ($\phi=-1$, -2, -4, -8, and -16). The results shown in Fig. 6(a) indicate that the exponent D_γ has an effective value of 1.69±0.02 for all five values of ϕ. Fig-

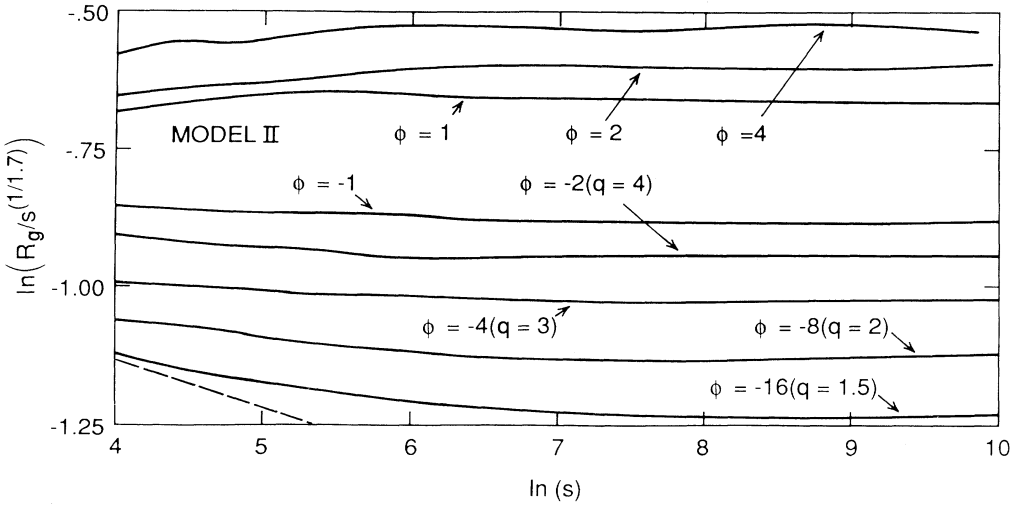

FIG. 5. The dependence of $\ln(R_g/s^{(1/1.7)})$ on $\ln(s)$ obtained from off-lattice model II clusters with eight different values for the exponent ϕ in Eq. (1). In those cases where a finite value for q was used that value is given in parentheses. In all cases 20 or more clusters were used to generate these results for each value of ϕ. For small cluster sizes slopes of -0.088 and 0.412 corresponding to $R_g\sim s^{1/2}$ and $R_g\sim s$, respectively, are expected for large negative and positive values of ϕ respectively. The dashed line has a slope of -0.088. The $R_g\sim s$ behavior cannot be seen in this figure but has been found for larger values of ϕ and/or smaller s.

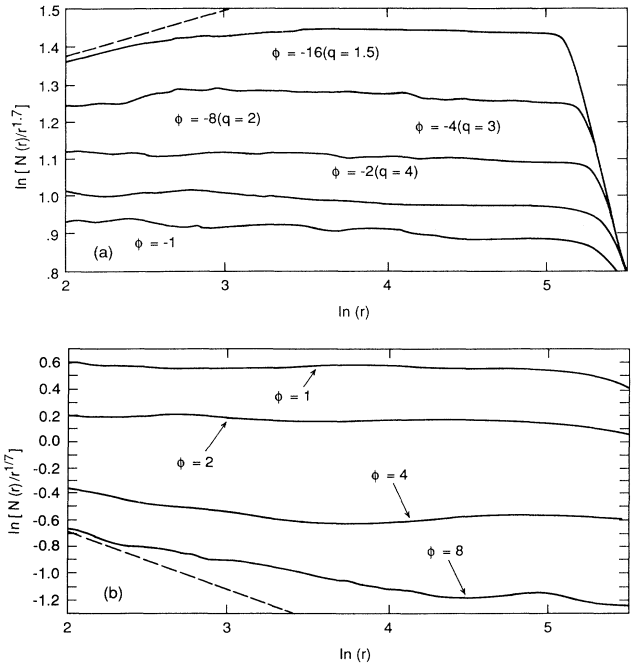

FIG. 6. The dependence of $\ln[N(r)/r^{1.70}]$ on $\ln(r)$ obtained using the off-lattice version of model II. (a) For five negative values of the radial bias exponent ϕ. The dashed line corresponds to the scaling $N(r)\sim s^2$ expected for $r<\mathcal{R}_x$. (b) Similar results for four positive values of ϕ. The dashed line corresponds to the scaling $N(r)\sim r$ expected for $r<\mathcal{R}_x$.

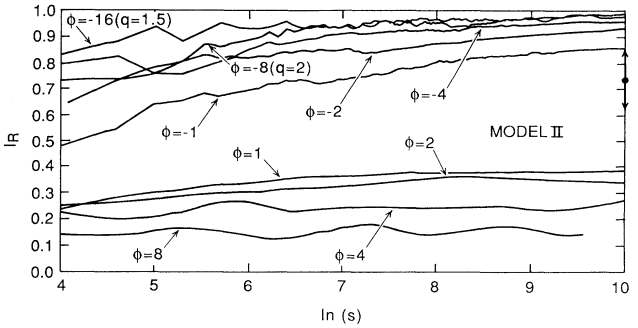

FIG. 7. Dependence of the mean value of the ratio I_R of the principal values of the inertial tensor (averaged over 20 clusters for each value of ϕ) on the cluster size s. Results are shown for model II using nine different values for the radial bias exponent ϕ. The double-headed arrow shows the value obtained from off-lattice DLA (Ref. 37) for clusters containing about 25 000 particles.

ure 6(b) shows the results of a series of simulations with positive values of ϕ. Now the statistical uncertainties are much larger but the results are also consistent with the idea that D_γ has an asymptotic value close to 1.70.

C. Cluster shape

It is apparent (particularly from Fig. 3) that as the value for the radial bias exponent ϕ is made more negative the cluster takes on a more round overall shape. Garick[37] has measured the overall shape anisotropy of off-lattice DLA clusters using the ratio of the cluster radii of gyration about the principal axes of the inertial tensor. Here we have measured the inertial tensor $\mathcal{I}$ of the clusters as a function of cluster size s. The elements of $\mathcal{I}$ are given by

$$\mathcal{I}_{ij}=\sum_{n=1}^{s}(\mathbf{r}_n-\langle\mathbf{r}\rangle)_i(\mathbf{r}_n-\langle\mathbf{r}\rangle)_j\ , \tag{4}$$

where $\langle\mathbf{r}\rangle$ is the position of the center of mass. The inertial tensor $\mathcal{I}$ is diagonalized and the quantity $I_R=\lambda_1/\lambda_2$ is calculated where λ_1 and λ_2 are the eigenvalues of $\mathcal{I}$ and $\lambda_2>\lambda_1$. Garick found that the ratio of the principal radii of gyration increased with increasing cluster size reaching a value of about 0.87 ± 0.07 ($I_R=0.76\pm0.12$) for clusters of size $s=50\,000$ particles. He concluded that the average radius of gyration ratio slowly approaches an asymptotic ($s\rightarrow\infty$) value of 1.0. However, it is not possible to determine from the simulation results alone if this ratio is exactly 1.0 or merely close to 1.0. Figure 7 shows the cluster size dependence of I_R obtained from simulations carried out using an off-lattice version of model II with nine different values for the radial bias exponent ϕ. Our results suggest that for $\phi\geq1$ the ratio I_R asymptotically approaches a limiting value that is neither 1 or 0 and that the limiting ratio I_R increases as ϕ decreases. For $\phi\leq-1$, I_R increases with increasing cluster size and has reached a value quite close to 1.0 for $s=25\,000$ particles. However, it is not clear if the asymptotic ($s\rightarrow\infty$) value for I_R is 1.0 or a value close to 1.0.

D. The active zone

For simple DLA models the growth of the width of the "active zone" (regions where growth is occurring). Δ, with increasing cluster size s can be described by the effective power law.

$$\Delta\sim s^{\nu}\ . \tag{5}$$

Plischke and Rácz[38] measured the exponent ν using relatively small clusters and found an effective value of about 0.48 ± 0.01 that is much smaller than the value of $1/D$ ($\simeq0.5888$ for $D=1.70$) expected for the growth of a homogeneous self-similar fractal with a fractal dimensionality of D. Larger-scale simulations,[35,39] however, indicate that the effective value of the exponent ν increases with increasing cluster size and most probably reaches an asymptotic value of $1/D$ as $s\rightarrow\infty$. Figure 8 shows the dependence of $\ln(\Delta/s^{(1./1.7)})$ on $\ln(s)$ obtained from model II clusters with seven different values for the radial bias exponent ϕ. For negative values of ϕ the effective value for the exponent ν in Eq. (5) is significantly smaller than $1/D$ (0.588) and for off-lattice model II clusters generated with $\phi=-16$ in the size range $100\leq s\leq10\,000$ the exponent ν has an effective value of about $0.588-0.21\simeq0.38$. We have not been able to carry out sufficiently many simulations to reduce statistical uncer-

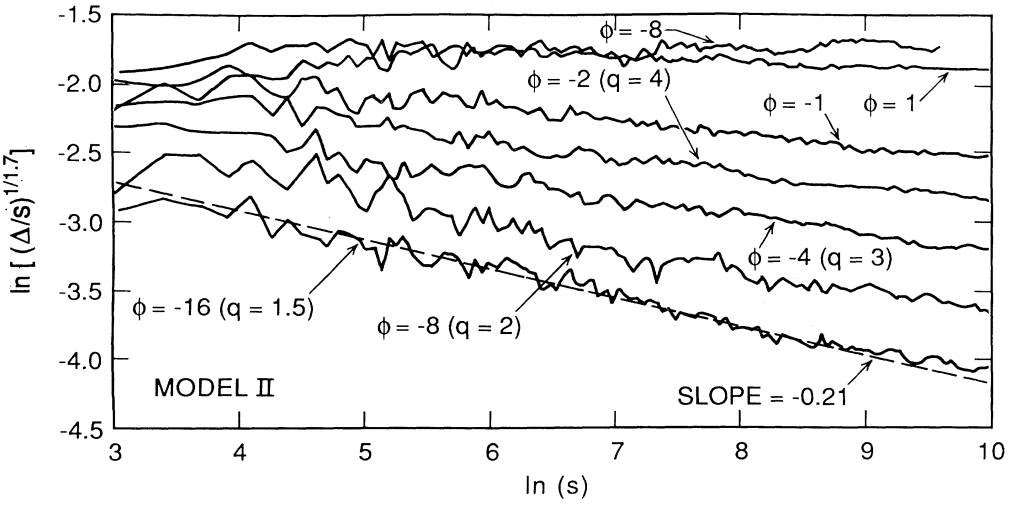

FIG. 8. Dependence of $\ln(\Delta/s^{(1/1.7)})$ on $\ln(s)$ obtained for seven values of the radial bias exponent ϕ for the off-lattice version of model II. Here Δ is the width of the active zone obtained from the mean difference between the deposition radii for successively added particles.

tainties to a level where the cluster size dependence of ν can be systematically explored. However, our results are consistent with the idea that the exponents ν and β describing the growth of the active zone and the radius of gyration converge to a common value that is equal to the asymptotic value of β for off-lattice DLA. To obtain the results given in Fig. 8 the width of the active zone, Δ, was obtained by calculating the quantity

$$\Delta = \langle\langle\, |(|\mathbf{r}_i| - |\mathbf{r}_{i+1}|)|\,\rangle\rangle\ , \tag{6}$$

where $\mathbf{r}_i$ is the distance measured from the cluster centers of mass at which the ith particle is deposited. The quantity $|(|\mathbf{r}_i| - |\mathbf{r}_{i+1}|)|$ is averaged over both a small increment in the growth of the cluster size ($s \rightarrow 1.05s$) and over a sample of (about 20) clusters.

E. Scaling in a strip geometry

Most of our simulations were carried out using off-lattice versions of model I and model II. However, qualitatively similar results were obtained using square-lattice models. Simulations were also carried out in "strip geometry" using periodic boundary conditions in the lateral direction. Figure 9 shows deposits of 4×10^5 sites grown on a square-lattice strip width 2048 lattice units with the parameters $\phi=-16$ ($q=1.5$) in Fig. 9(a), $\phi=-8$ ($q=2.0$) in Fig. 9(b), and $\phi=-4$ ($q=3.0$) in Fig. 9(c). In this model the growth probability at position $\mathbf{r}$ is given by

$$P(\mathbf{r}) \sim \mu(\mathbf{r}) h^{\phi}\ , \tag{7}$$

where h is the y coordinate of $\mathbf{r}$ measured from the linear "substrate." The density profiles obtained from these simulations are shown in Fig. 10. It is apparent that over a substantial range of length scales (more than two decades) the density profile can be described quite well by the simple power-law form

$$\rho(h) \sim |\phi|^{(2-D)} h^{-\alpha}\ , \tag{8}$$

where $\rho(h)$ is the mean density at a height of $h = y - y_0$. For $\phi=-16$ exponent α has a value of about 0.35. The value obtained for α appears to decrease as ϕ increases from -16 to 0 (DLA) and our results are consistent with the value of 0.28 found for the ordinary DLA model.[40] While this observation might be taken as an indication of nonuniversality we believe that the apparent variation in α over the range $-16<\phi<0$ is smaller than the combined uncertainties due to finite size and statistical effects. To test the hypothesis that α is indeed independent of ϕ might be a direction for future (massive) simulations.

It appears that the density profile can be described in terms of a fractal dimensionality $D_\alpha = d - \alpha$ that is approximately equal to the fractal dimensionality D_β obtained from the growth of the radius of gyration.

Figure 11 shows the density correlation functions in the lateral x direction at several heights h for deposits generated with bias exponents ϕ of -4 [Fig. 11(a)] and -16 [Fig. 11(b)]. Here the correlation function $C_h(x)$ is defined as

$$C_h(x) = \frac{1}{L} \sum_{x'=1}^{L} \rho(h,x')\rho(h,x'+x)\ , \tag{9}$$

where $\rho(h,x)$ is the deposit density at height h and lateral position x. In practice the quantity $\rho(h,x)$ was averaged over a small height range.

At short length scales x this correlation function appears to have a power-law form

$$C_h(x) \simeq x^{-\nu}\ , \tag{10}$$

with an effective exponent ν of about $\frac{1}{2}$.

IV. DISCUSSION

At the onset of this work we had expected that the introduction of a power-law radial bias might be sufficient to change the geometric scaling properties. This impression was strengthened by the appearance of the clusters shown in Figs. 1–3. In these models the growth probability measure can be written in the form $\mu(\mathbf{r})l^{\phi}$ where $\mu(\mathbf{r})$ is the harmonic measure and l is either Pythagorean distance or minimum path distance at $\mathbf{r}$ to the seed or origin of the cluster. Consequently, it was initially surprising to find that the exponents $\beta=1/D_{\beta}$ and D_{γ} were unchanged for all values of ϕ. There are, however, crossover effects visible at small cluster sizes as discussed below.

It is not surprising that models I and II in Eq. (1) give

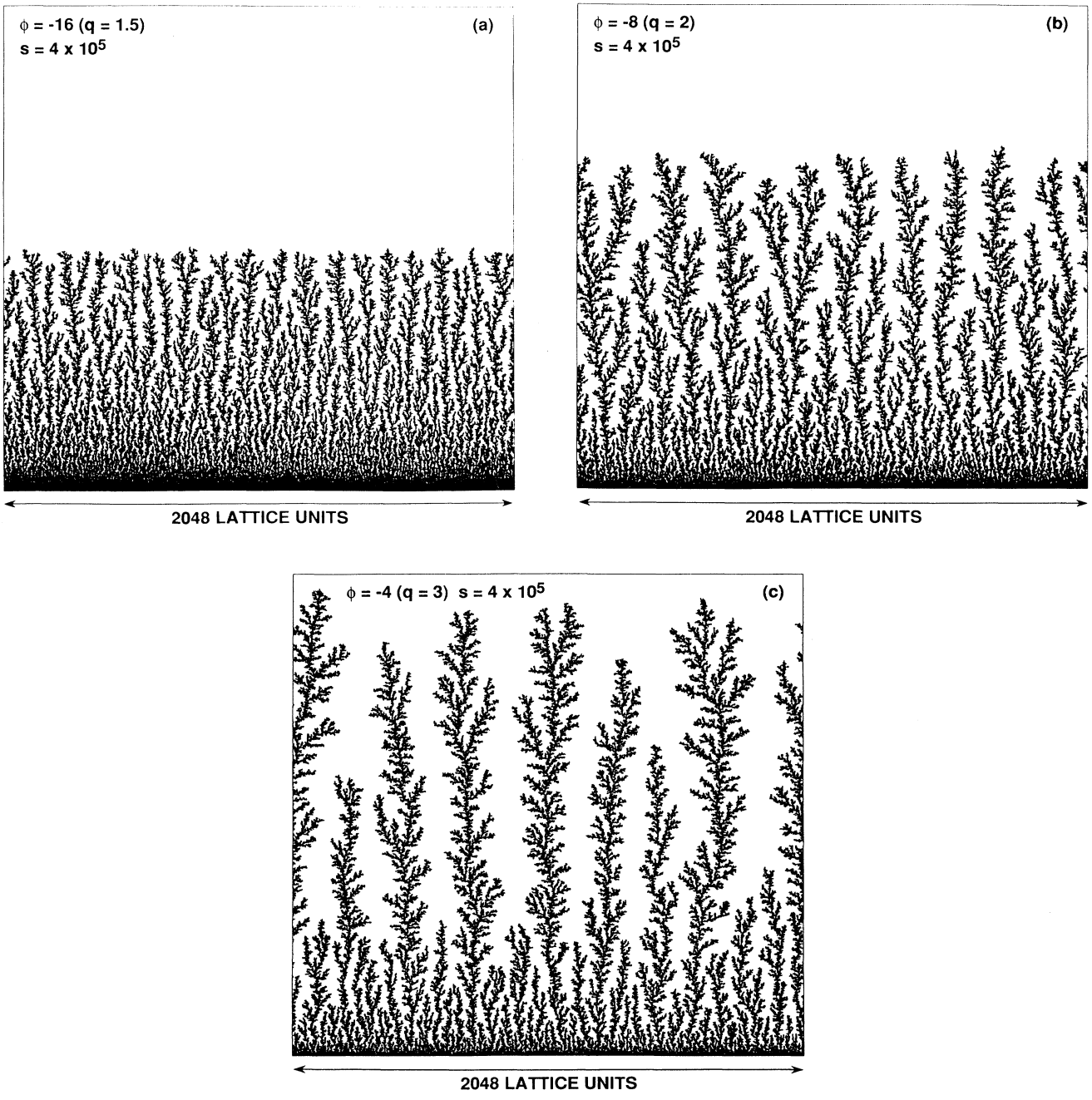

FIG. 9. Deposits consisting of 4×10^5 sites grown on strips of width $L=2048$ lattice units from a linear substrate. Results are shown for (a) $-\phi=-16$ ($q=1.5$); (b) $-\phi=-8$ ($q=2$); (c) $-\phi=-4$($q=3$).

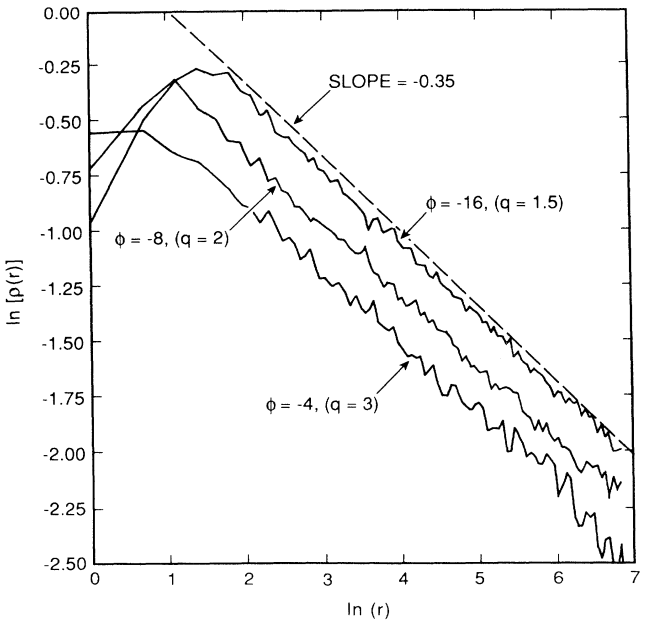

FIG. 10. Density profiles obtained from the simulations shown in Fig. 9. The initial increase in the density $\rho(h)$ with increasing height, h, for $\phi=-8$ and -16 is a consequence of the finite value used for the parameter q. For heights h, greater than about 5 lattice units this effect becomes negligible.

very similar results since the exponent $D_{\min}$ relating r and d,

$$d(r)\sim r^{D_{\min}} , \tag{11}$$

has a value[41] of 1. Here d is the minimum path distance and r is the Pythagorean distance measured in the Euclidean embedding space. Although $D_{\min}$ was not measured for the models used in this work, it seems most likely that $D_{\min}$ is 1 for these models also. This seems particularly evident for clusters such as that shown in Fig. 3 that have been generated using large negative values for the radial bias exponent ϕ.

The correlation length ξ

Perturbations of fractal growth models generally introduce new length scales that characterize the crossover between different scaling regimes. We find that the introduction of the radial bias exponent introduces geometric changes in the DLA structure. The DLA structure itself has several length scales. The fundamental length is the particle diameter $a=1$. The other length scale of DLA is the overall size of the cluster as given by radius of gyration R_g or the maximal diameter of the cluster.

Self-similar fractal structures have no length scale apart from the small-scale (particle size) and large-scale (cluster size) cutoff lengths. However, the self-similarity of DLA has been under discussion for some time and is not entirely clarified. In particular it remains an open question to what extent one may say that DLA is a self-similar fractal.

The distance ξ over which the bias function $b(r)=l^{\phi}$ changes by a significant amount is given by

$$\left|\xi\frac{1}{b(r)}\frac{db(r)}{dl}\right|\simeq 1\Longrightarrow\xi=\frac{l}{|\phi|} , \tag{12}$$

so that ξ has a value that is proportional to $|\phi|^{-1}$ and diverges as the DLA limit, $\phi=0$, is approached. This means that the cluster is expected to have a structure essentially that of an unbiased DLA on length scales up to a length ξ equal to $l/|\phi|$. It appears from Fig. 3(a) and the simulations carried out using strip geometry that the structure is essentially uniform for negative ϕ on longer length scales. The length ξ corresponds roughly to the width of the main branches in the clusters. For $\phi\ll -1$, this width also corresponds to the spacing between the

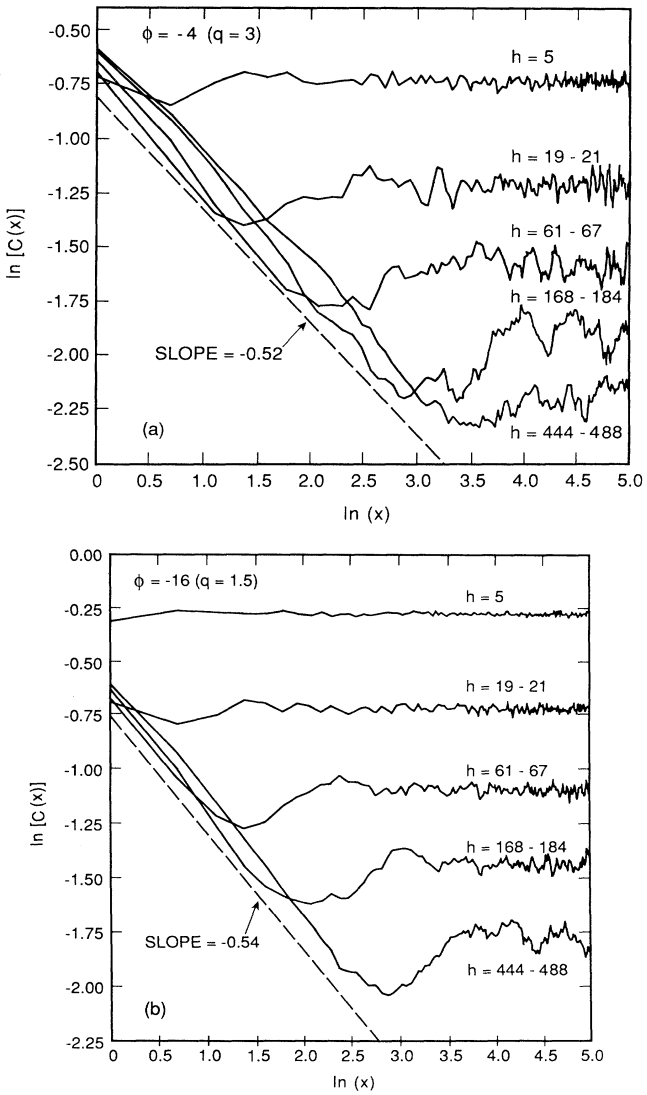

FIG. 11. Lateral correlation functions $C_h(x)$ obtained from simulations shown in Fig. 9(a). The correlation functions for $\phi=-4$ and $q=3$ at five height ranges. (b) The results for $\phi=-16$ and $q=1.5$ at the same heights.

main branches. This spacing increases with increasing distance l from the seed since $\xi \sim l$.

The fact that the clusters have the same scaling structures as DLA up to length scales ξ can be expressed in terms of crossover functions. It turns out that the visually very different behavior observed for positive and negative values of the radial bias exponent ϕ is reflected in separate scaling functions that are discussed below.

In the extreme limit $\phi \gg 1$, the cluster will grow only at the most distant tip producing a linear structure (this has been demonstrated explicitly in computer simulations carried out using values as large as 512 for the exponent ϕ). This will continue until the correlation length $\xi = l/|\phi|$ becomes of the order of 1. This occurs when l is of the order of $\mathcal{R}_x = |\phi|$. Thus the radial bias exponent leads to an increased lower cutoff since the single-particle steric constraints now extend to $\mathcal{R}_x = a|\phi|$, where $a = 1$ is the particle diameter. For distances much greater than $\mathcal{R}_x$ the cluster will have a finite width approximately equal to the correlation length which increases with distance leaving a wedge-shaped structure [see Fig. 3(b)]. The structure inside the wedge is like that of DLA. As a consequence the mass in the wedge per unit length at a distance l from the origin will be proportional to ξ^{D-1}. Therefore a cluster of maximal extent l_m will have a mass scaling given by

$$s \sim \int_0^{l_m} \left[\frac{l}{|\phi|} \right]^{D-1} dl \sim |\phi|^{-(D-1)} l_m^D \ . \tag{13}$$

Since the radius of gyration is proportional to l_m we conclude that the radius to gyration will asymptotically scale as

$$R_g = R_+ |\phi|^{(D-1)/D} s^{1/D} \ . \tag{14}$$

This result is consistent with Eq. (2), and we conclude that $\beta = 1/D$, for positive values of the radial bias exponent ϕ. For small values of s there are deviations from this scaling behavior as shown in Fig. 5. For $\phi > 0$ the behavior is consistent with $R_g \sim s$ for small s as expected.

For large positive values of ϕ the wedge-shaped cluster has a DLA-like structure on length scales δ smaller than $\xi = l/\phi$. The mass density up to $\delta \simeq \xi$ is $\rho = \xi^D/\xi^2 = \xi^{(D-1)}$. The mass per unit length of this structure is then $\rho \xi dl$ provided $l > \mathcal{R}_x$. For $l < \mathcal{R}_x$ the mass increases linearly with l. The number of particles inside a radius r will scale as $N(r) \sim r$ for $r < \mathcal{R}_x$ and $N(r) \sim r^D$ for $r > \mathcal{R}_x$ as just discussed. This behavior may be summarized as follows:

$$N(r) \sim r \mathcal{F}_+(r/\mathcal{R}_x) \rightarrow \begin{cases} r, & r < \mathcal{R}_x \\ (1-N_+)\mathcal{R}_x + N_+ |\phi|^{(1-D)} r^D, & r > \mathcal{R}_x \end{cases} \quad \text{for } \phi \gg 1 \ . \tag{15}$$

Here the scaling function $\mathcal{F}_+(x)$ has the form $\mathcal{F}_+(x) \sim x^{-\nu_+}$ with $\nu_+ = D-1$ for $x \gg 1$ and $\mathcal{F}_+(x) \sim$ const for $x < 1$. This crossover is consistent with the results shown in Fig. 6 where we find a crossover to $N(r) \sim r$ for small r.

Arian *et al.*[42] have discussed a modification of the dielectric breakdown model where only growth with $\mu(\mathbf{r}) > \mu_c$ is allowed. This modification favors growth at the tips and Arian *et al.* find a crossover from DLA on short length scales to a new spiky behavior (at large sizes) that looks quite different from the wedge-shaped structures we find for $\phi \gg 1$. The crossover radius R_x is proportional to $1/\mu_c$.

From Eq. (15) it follows that we expect the following scaling for the *amplitude* $N_0(\phi)$ in Eq. (3):

$$N_0(\phi) = N_+ |\phi|^{\nu_+} \quad \text{with } \nu_+ = 1 - D_\gamma \quad \text{for } \phi \gg 1 \ . \tag{16}$$

As already discussed the data in Fig. 6(b) show that $N(r)$ indeed exhibits the r^{D_γ} scaling assumed as a basis for Eq. (15). Figure 12 shows the amplitudes $\ln[N_0(\phi)]$ (from Fig. 6) as a function of $\ln(|\phi|)$. Figure 12 shows a fit of Eq. (16) to the results of the simulations. The effective value obtained for the exponent ν_+ from the largest $|\phi|$ values in the data shown in Fig. 6(b) is about $\nu_+ \simeq -0.90$, in reasonable agreement with the value of $(1-D)$ or about -0.70 predicted by Eq. (16). Clearly the asymptotic regime of large ϕ has not been reached for the values $\phi = 4$ and 8 used in the estimate of ν_+.

The wedge-shaped structure is a self-affine structure in the sense that if one determines the box counting dimension by covering the structure with boxes of size δ one finds that the the number of boxes needed to cover the structure is $N(\delta) \sim \delta^{-D}$ for $\delta \ll \xi_{\max} = l_{\max}/\phi$, but

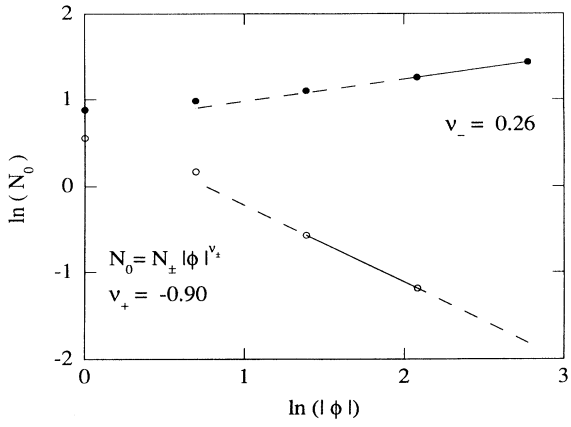

FIG. 12. Dependence of the amplitude $N_0(\phi)$ on the bias function exponent ϕ obtained from the data shown in Fig. 7.

$N(\delta)\sim\delta^{-1}$ on long length scales $\delta>\xi_{\max}$. Therefore we have the usual result for self-affine structures, namely, that one has to distinguish between the local and the global fractal dimension. The wedge-shaped branches are globally one dimensional or "linear."

Clusters grown with negative values of the radial bias exponent also have interesting scaling properties. Using the notion that the clusters have the DLA structure anywhere in the cluster up to the length scale ξ, then the number of points inside a circle of radius ξ is ξ^D and therefore the mean density $\rho(r)$ at a distance r from the substrate or seed is given by

$$\rho(r)\sim\xi^{D-2}\sim(l/|\phi|)^{-\alpha}\ , \tag{17}$$

where α is the fractal codimension for DLA ($\alpha=d-D_\alpha\sim0.3$, where D is the fractal dimensionality). According to this picture we expect to find that the power-law shape of the density profile and the growth of the radius of gyration can be described by the exponent that describe the same quantities in DLA. In this sense the models described here and DLA belong to the same universality class.

In the extreme limit $\phi\ll-1$, the cluster will initially grow as closely to the center as possible producing a dense two-dimensional structure. This will continue until the correlation length $\xi=l/|\phi|$ becomes of the order of 1, which occurs when l is of the order of $\mathcal{R}_x=|\phi|$:

$$1=\xi=\mathcal{R}_x/|\phi|\Longrightarrow\mathcal{R}_x=|\phi|\ . \tag{18}$$

Thus also in this case the radial bias exponent leads to an increased lower cutoff since the single-particle steric constraints now extend to $\mathcal{R}_x=a|\phi|$, where $a=1$ is the particle diameter, and the particle density given in Eq. (17) is valid only for $r\gg\mathcal{R}_x$. As shown in Fig. 5 we find that the scaling $R_g\sim s^2$ is approached for small cluster masses s in the case $\phi\ll-1$.

Thus we expect a crossover for $N(r)$ from $N(r)\sim r^2$ for $r\ll\mathcal{R}_x$ to $N(r)\sim r^D$ for $r\gg\mathcal{R}_x$ controlled by a scaling function $\mathcal{F}_-$:

$$N(r)\sim r^2\mathcal{F}_-(r/\mathcal{R}_x)\rightarrow\begin{cases}r^2, & r<\mathcal{R}_x\\ (1-N_-)\mathcal{R}_x^2+N_-|\phi|^{(2-D)}r^D, & r>\mathcal{R}_x\text{for }\phi\ll-1\ .\end{cases} \tag{19}$$

Here the scaling function $\mathcal{F}_-(x)$ has the form $\mathcal{F}_+(x)\sim x^{-\nu}$ for $x\gg1$ and $\mathcal{F}_-(x)\sim$const for $x<1$. In order to obtain the correct limit for small r we conclude that we have $\nu_-=2-D$. From Eq. (19) it follows that the amplitude $N_0(\phi)$ in Eq. (3) has a power-law dependence on the radial bias exponent:

$$N_0(\phi)=N_-|\phi|^{\nu_-}\ \text{ with }\nu_-=2-D_\gamma\ \text{ for }\phi\ll-1\ . \tag{20}$$

A fit of this relation to the amplitudes obtained in simulations (see Fig. 6) is shown in Fig. 12. The effective value for $\nu_-\simeq0.26$, which is consistent with the expected value $2-D=0.3$. The crossover to a compact core described by Eq. (19) is consistent with the result shown in Fig. 6 where we find a beginning of a crossover to $N(r)\sim r^2$ for small r and $\phi\ll-1$.

Arguments similar to those used to obtain Eq. (19) can be used to calculate the exponent σ_- describing the dependence of the amplitude $R_0(\phi)$ in Eq. (2) on ϕ. In this case it follows directly from Eq. (19) that the exponent σ_- defined below is related to ν_- by

$$R_0(\phi)=R_-|\phi|^{\sigma_-}\ \text{ with }\sigma_-=-\nu_-/D\ , \tag{21}$$

or $\sigma_-\simeq-0.176$ for $D=1.70$. From the results shown in Fig. 5(a) a value of about -0.14 is obtained for the effective value of σ_-. For positive values of the radial bias exponent ϕ, there is no simple relation between the scaling of the amplitude of the radius of gyration R_0 and the amplitude N_0 in Eq. (3) for $\phi\gg1$ since in this case the growing cluster crosses over to an inhomogeneous self-affine structure and the center of mass and the origin grow far apart (Fig. 2).

The density profiles in the strip geometry (see Fig. 10) can be understood in terms of a similar model. Here we expect that the density profile $\rho(r)$ is given by Eq. (17) so that the density should have values proportional to $\xi^{-\alpha}$. This implies that the dependence of $\ln[\rho(h)]$ on $\ln(h)$ for values of ϕ differing by a factor of 2 should consist of parallel straight lines with slope $-\alpha$ separated by a distance of $\ln(2^\alpha)$ or 0.208. The results shown in Fig. 10 are consistent with these ideas. These results and the scaling form proposed in Eq. (8) suggest that it might be possible to express all the lateral correlating functions for different values of h and ϕ in terms of the simple scaling form in terms of the length scale $\xi=h/|\phi|$:

$$C_h(x)\simeq\xi^{-\alpha}g(x/\xi^{\alpha/\nu})\ , \tag{22}$$

where the scaling function $g(x)$ has the form $g(x)\simeq x^{-\nu}$ for $x\ll1$ and $g(x)\sim$const for $x\gg1$. This idea is tested in Fig. 13. Figure 13(a) shows the correlation function $C_h(x)$ obtained from simulations with $\phi=-4$, -8, and -16 averaged over the height ranges $h=19$–20, 61–67, and 168–184. Figure 13(b) shows the data collapse obtained using the scaling form given in Eq. (22) using values of $\frac{1}{3}$ for α and $\frac{1}{2}$ for ν. The data collapse is quite good and lends strong support to the scaling form given in Eq. (22).

The results obtained from the strip geometry simulations for deposition on a line are fully consistent with the strip geometry DLA simulations of Meakin and Family[43] and the more recent work of Evertsz[44] using dielectric breakdown models that both indicate that the deposit structure has self-affine scaling properties.

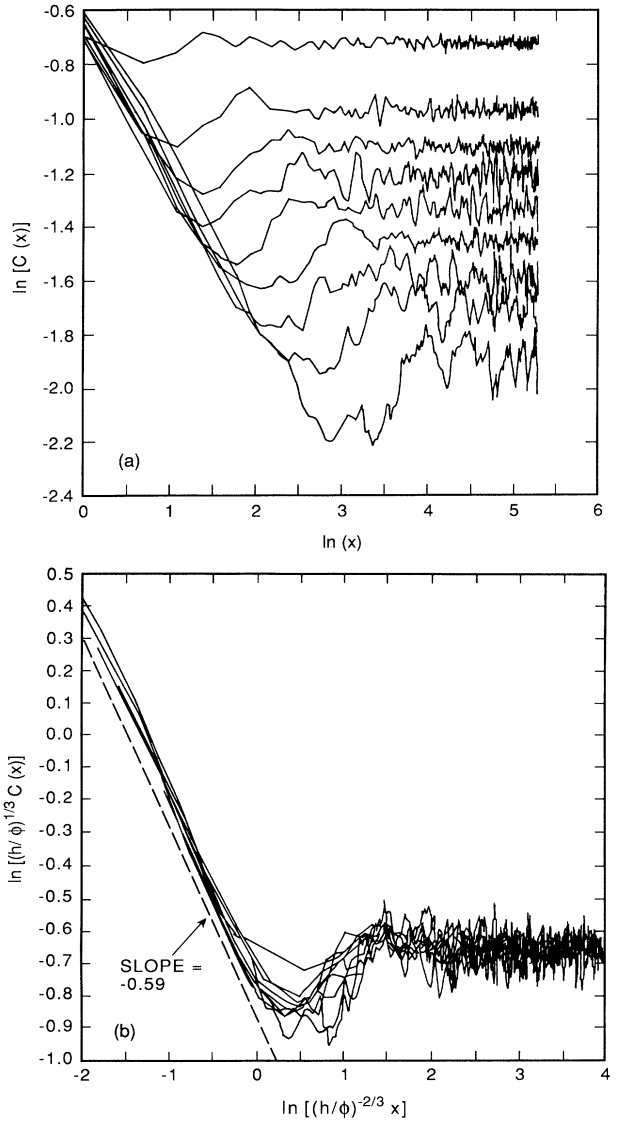

FIG. 13. Scaling of the lateral correlation functions. (a) shows the correlation functions $C_h(x)$ obtained using the parameters $\phi=-4$ ($q=3$), $\phi=-8$ ($q=2$), $\phi=-16$ ($q=1.5$) at three different height ranges. (b) shows how these correlation functions can be scaled using the scaling form given in Eq. (22). In (b) the height h represents the mean height for each of the three narrow ranges.

The introduction of a power-law radial bias acceptance characterized by an exponent ϕ can be considered to a be perturbation of the DLA model. This perturbation introduces a length scale ξ that diverges at the DLA point. This behavior is reminiscent of the behavior at second-order phase transitions where the correlation function ξ diverges at the critical temperature but remains finite both above and below the phase transition. The structural change caused by the radial bias function $b(r)\sim l^{\phi}$ is analogous to a second-order structural phase transition and the radial bias exponent ϕ plays a role analogous to the reduced temperature in phase transitions. In the language of renormalization group theory we might say that the perturbation $b(r)$ is a relevant perturbation of the DLA model. However, such an analogy is limited in that we have no property analogous to the order parameter that distinguishes the ordered phase from the disordered phase in ordinary phase transitions. The "phase" found for $\phi<1$ is characterized by having a dense nonfractal core with a radius given by $\mathcal{R}_x\sim|\phi|$. In the $\phi>0$ "phase" there is a "linear" structure up to the length scale $\mathcal{R}_x$, which develops into a wedge-shaped self-affine structure. In this analogy the DLA structure represents the *critical point* of the class of models discussed here. It is interesting to note that the fact that N_0 exhibits a better scaling with $\phi-1$ (see Fig. 12) than with ϕ is similar to the experience from phase transitions where extrapolations based on observations far from the critical point give a wrong estimate of the transition temperature and where renormalization effects change the behavior near the critical point.

From this point of view it is perhaps not surprising that the geometrical structure of DLA has been so difficult to clarify since it represents the critical point in a "geometrical phase transition." Computer simulations indicate that in DLA itself the structure is also inhomogeneous with the seed origin being at the center or a region of anomalously high density but still having fractal scaling. The DLA structure may be analyzed in terms of a hierarchy of branch orders of decreasing length. The conclusion from such an analysis[45,46] is that DLA is in a state of geometrical crossover where branches of a given order have a characteristic length L_n that depend on the branch order. Branches of order n are essentially linear on length scales $\delta<L_n$, whereas these branches are fractally distributed over the cluster on length scales $\delta\gg L_n$. Simulations also indicate that the density correlations in the angular (tangential) direction are quite different from the density correlations in the radial direction.[47,48] These characteristics are exhibited quite dramatically by the clusters grown with a radial bias exponent of -32 in Fig. 3. We speculate that DLA itself represents the geometric analog of a critical point in phase transitions that is essentially of a self-similar structure. The clusters such as that shown in Fig. 3 may be helpful in understanding the structure of DLA and other related growth models.

ACKNOWLEDGMENTS

The work in Olso was supported by VISTA, a research cooperation between the Norwegian Academy of Science and Letters and Den norske stats oljeselskap a.s. (Statoil), and by NAVF—the Council of Natural Science Research.

[1]T. A. Witten and L. M. Sander, Phys. Rev. Lett. **47**, 1400 (1981).
[2]T. Vicsek, *Fractal Growth Phenomena* (World Scientific, Singapore, 1989).
[3]J. Feder, *Fractals* (Plenum, New York, 1988).
[4]P. Meakin, in *Phase Transitions and Critical Phenomena,* edited by C. Domb and J. L. Lebowitz (Academic, New York, 1987), pp. 336–489.
[5]*The Fractal Approach to Heterogeneous Chemistry,* edited by D. Avnir (Wiley, Chichester, 1989).
[6]*Fractals in Physics: Essays in Honour of Benoit B. Mandelbrot,* edited by A. Aharony and J. Feder (North-Holland, Amsterdam, 1989).
[7]*Fractals in the Natural Sciences,* Proceedings of the Royal Society, London, 1988, edited by M. Fleischmann, D. J. Tidesley, and R. C. Ball [Proc. R. Soc. London **423**, 1 (1989)].
[8]*On Growth and Form: Fractal and Nonfractal Patterns in Physics,* edited by H. E. Stanley and N. Ostrowsky (Nijhoff, Dordrecht, 1986).
[9]*Fractals in Physics,* edited by L. Pietronero and E. Tosatti (North-Holland, Amsterdam, 1986).
[10]*Phase Transitions in Soft Condensed Matter,* edited by T. Riste and D. Sherrington (Plenum, New York, 1989).
[11]B. B. Mandelbrot, *The Fractal Geometry of Nature* (Freeman, New York, 1982).
[12]D. G. Grier, D. A. Kessler, and L. M. Sander, Phys. Rev. Lett. **59**, 2315 (1987).
[13]Y. Sawada, A. Dougherty, and J. P. Gollub, Phys. Rev. Lett. **56**, 1260 (1986).
[14]D. Grier, E. Ben Jacob, R. Clarke, and L. M. Sander, Phys. Rev. Lett. **56**, 1264 (1986).
[15]H. Fujikawa, and M. Matsushita, J. Phys. Soc. Jpn. **58**, 3875 (1989).
[16]E. Ben Jacob, G. Deutscher, P. Garik, N. D. Goldenfeld, and Y. Lareah, Phys. Rev. Lett. **57**, 1903 (1986).
[17]A. Buka and A. Palffy-Muhoray, Phys. Rev. A **36**, 1527 (1987).
[18]L. Niemeyer, L. Pietronero, and H. J. Wiesmann, Phys. Rev. Lett. **57**, 650 (1986).
[19]P. Garik, E. Ben Jacob, E. Bochner, N. Broxholm, B. Miller, B. Orr, and R. Zamir, Phys. Rev. Lett. **62**, 2703 (1989).
[20]A. T. Skjeltorp and G. Helgesen, in *Phase Transitions in Soft Condensed Matter,* edited by T. Riste and D. Sherrington (Plenum, New York, 1989), pp. 23–43.
[21]H. van Damme, in *The Fractal Approach to Heterogeneous Chemistry,* edited by D. Avnir (Wiley, Chichester, 1989), pp. 199–226.
[22]D. B. Hibbert and J. R. Melrose, Phys. Rev. A **38**, 1036 (1988).
[23]J. Nittmann and H. E. Stanley, Nature (London) **321**, 663 (1986).
[24]T. Vicsek, Phys. Rev. Lett. **53**, 2281 (1984).
[25]T. Vicsek, Phys. Rev. A **32**, 3084 (1985).
[26]J. Nittmann and H. E. Stanley, J. Phys. A **20**, L981 (1987).
[27]F. Family, D. E. Platt, and T. Vicsek, J. Phys. A **20**, L177 (1987).
[28]P. Meakin, F. Family, and T. Vicsek, J. Colloid Interface Sci. **117**, 394 (1987).
[29]R. F. Xiao, J. Iwan, D. Alexander, and F. Rosenberger, Phys. Rev. A **38**, 2447 (1988).
[30]T. Hepel, J. Electrochem. **134**, 2685 (1987).
[31]L. M. Sander, P. Ramanlal, and E. Ben Jacob, Phys. Rev. A **32**, 3160 (1985).
[32]R. F. Voss, Phys. Rev. B **30**, 334 (1984).
[33]P. Meakin, and J. M. Deutch, J. Chem. Phys. **80**, 2115 (1984).
[34]P. J. Meakin, Theor. Biol. **118**, 101 (1986).
[35]P. J. Meakin, J. Phys. A **17**, 473 (1984).
[36]S. Tolman and P. Meakin, Phys. Rev. A **40**, 428 (1989).
[37]P. Garik, Phys. Rev. A **32**, 1275 (1985).
[38]M. Plischke and Z. Rácz, Phys. Rev. Lett. **53**, 415 (1984).
[39]P. Meakin and L. M. Sander, Phys. Rev. Lett. **54**, 2053 (1985).
[40]P. Meakin, J. Kertesz, and T. Vicsek, J. Phys. A **21**, 1271 (1988).
[41]P. Meakin, I. Majid, S. Halvin, and H. E. Stanley, J. Phys. A **17**, L975 (1984).
[42]E. Arian, P. Alstrøm, A. Aharony, and H. E. Stanley, Phys. Rev. Lett. **63**, 2005 (1989).
[43]P. Meakin and F. Family, Phys. Rev. A **34**, 2558 (1986).
[44]C. Evertsz, Phys. Rev. A **41**, 1830 (1990).
[45]E. L. Hinrichsen, K. J. Måløy, J. Feder, and T. Jøssang, J. Phys. A **22**, L271 (1989).
[46]J. Feder, E. L. Hinrichsen, K. J. Måløy and T. Jøssang, in *Fractals in Physics,* edited by A. Aharony and J. Feder (North-Holland, Amsterdam, 1989), pp. 104–111.
[47]P. Meakin and T. Vicsek, Phys. Rev. A **32**, 685 (1985).
[48]M. Kolb, J. Phys. (Paris) **46**, L631 (1985).